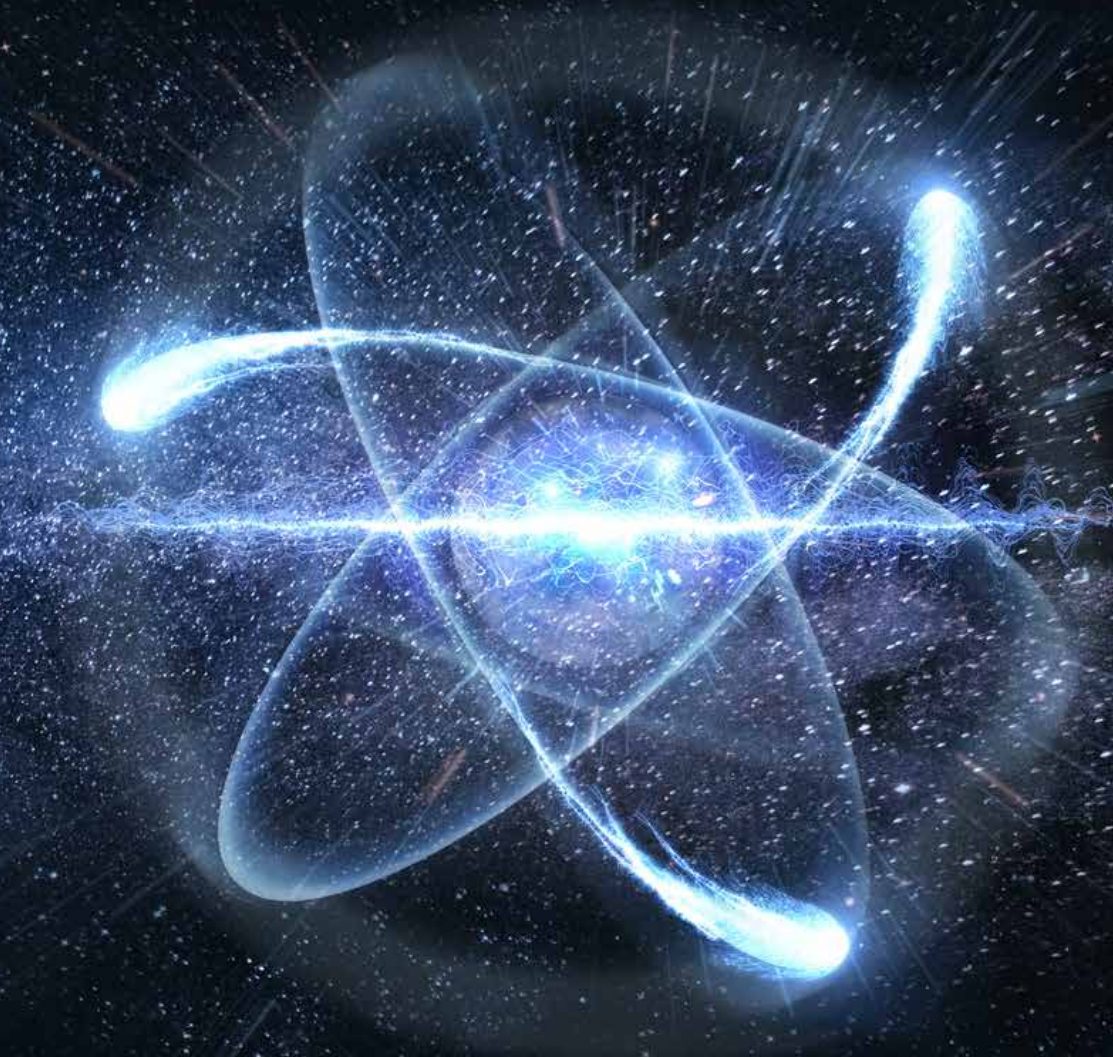


ESARDA BULLETIN

The International Journal of Nuclear Safeguards
and Non-Proliferation



ISSN 1977-5296
KJ-BB-22-002-EN-N

Volume 64 n.2
December 2022

Editor

Elena Stringa

Assistant Editor

Andrea De Luca

European Commission, Joint Research Centre,
Directorate G - Nuclear Safety and Security
Nuclear Security Unit G.II.7
T.P. 800, I-21027 Ispra (VA), Italy
Tel. +39 0332-786182
EC-ESARDA-BULLETIN@ec.europa.eu

ESARDA is an association formed to advance and harmonize research and development for safeguards. More information can be found at the following address:

<https://esarδα.jrc.ec.europa.eu/>

Editorial Board

K. Axell (SSM, Sweden)
K. Aymanns (FZJ, Germany)
S. Cagno (EC, JRC, J.1, Italy)
A. De Luca (consultant at EC, JRC, G.II.7, Italy)
S. Grape (UU, Sweden)
T. Krieger (FZJ, Germany)
O. Okko (STUK, Finland)
I. Popovici (CNCAN, Romania)
G. Renda (EC, JRC, G.II.7, Italy)
A. Rezniczek (Uba GmbH, Germany)
R. Rossa (SCK-CEN, Belgium)
J. Rutkowski (SNL, USA)
Z. Stefánka (HAEA, Hungary)
E. Stringa (EC, JRC, G.II.7, Italy)
A. Tomanin (DG ENER, Luxembourg)

Papers submitted for publication are reviewed by independent authors including members of the Editorial Board.

Manuscripts have to be sent to the Editor (EC-ESARDA-BULLETIN@ec.europa.eu) following the paper guidelines available in the ESARDA Bulletin section of the ESARDA website (<https://esarδα.jrc.ec.europa.eu/>) where the bulletins can also be viewed and downloaded.

Accepted manuscripts are published free of charge.

N.B. Articles and other material in the ESARDA Bulletin do not necessarily present the views or policies of neither ESARDA nor the European Commission.

ESARDA Bulletin is published jointly by ESARDA and the Joint Research Centre of the European Commission.

The publication is authorised by ESARDA.

© Copyright is reserved, but part of this publication may be reproduced, stored in a retrieval system, or transmitted in any form or by any means, mechanical, photocopy, recording, or otherwise, provided that the source is properly acknowledged.

Cover design and layout by Christopher Craig Havenga, (consultant at EC, JRC, G.II.7, Italy).



ESARDA BULLETIN

The International Journal of Nuclear Safeguards
and Non-Proliferation

Contents: Volume 64, n.2

Editorial

Elena Stringa 1

Peer Reviewed Articles

Impact of Concrete Building Structures on Neutron Radiation and its Mitigation 2
Svenja Sonder, Simon Hebel, Carina Prünte, Gerald Kirchner

Integration of independent NDA techniques within a SLAM-based robotic system for improving safeguards standard routines: a review of the current status and possible future developments 10
Filippo Gagliardi

Editorial

Elena Stringa

Dear Readers,

It is with pleasure that I present the second issue of volume 64 of the 'ESARDA Bulletin - The International Journal of Nuclear Safeguards and Non-proliferation'.

This volume is very light, containing only two contributions, both very interesting. The first paper deals with Arms Control and Disarmament Verification, in particular analyzing the impact of concrete building structures on the neutron radiation. The second published contribution is a review paper presenting the integration of independent NDA techniques within a SLAM-based robotic system for improving safeguards standard routines. This paper also discusses possible future developments, introducing interesting scenarios that can be of inspiration for the Safeguards community.

I would like to thank the authors for their interest in publishing their findings in our journal, and the reviewers for their hard work, that lead to the publication of high quality articles.

Please let me remind you that the ESARDA Bulletin is now a rolling publication. Articles can be submitted on a continuous basis and will be published online with their DOI as soon as they are ready, usually between 4 and 8 weeks after the submission.

If you wish to publish your work in the ESARDA Bulletin, send your article at any time together with the paper submission form duly filled and signed to EC-ESARDA-BULLETIN@ec.europa.eu. If accepted, the article will be published as soon as the review process will be completed.

Before submitting your work, please ensure that your paper fits the Bulletin scope and that its content presents some novelties: we do not accept work that has already been published in other journals or conference proceedings, unless new aspects of the work are introduced (e.g. new results and related discussion). You can find the publication policies in the ESARDA Bulletin website under documents and forms.

Before concluding, I would like to thank Andrea De Luca (assistant editor) for all the work done to improve our journal and all the work he's doing in registering DOIs for the single articles and for the ESARDA Bulletin website. Thank you also to Guido Renda and Simone Cagno for their valuable advices: their suggestions allowed to increase the quality of the journal. Finally, thank you to Christopher Haviga, our graphic designer, who has designed the Bulletin cover and edits all the articles to fit the publication layout, and to Lenka Hubert for all the support provided.

Enjoy the reading,

Dr. Elena Stringa, PhD

Editor of the ESARDA Bulletin - The International Journal of Nuclear Safeguards and Non-Proliferation
EC-ESARDA-BULLETIN@ec.europa.eu
https://esarda.jrc.ec.europa.eu/publications-0/esarda-bulletin_en

Impact of Concrete Building Structures on Neutron Radiation and its Mitigation

Svenja Sonder, Simon Hebel, Carina Prünke, Gerald Kirchner

Carl-Friedrich von Weizsäcker-Zentrum für Naturwissenschaft und Friedensforschung, Universität Hamburg, Beim Schlump 83, 20144 Hamburg

E-mail: svenja.sonder@uni-hamburg.de

Abstract:

A key technique for nuclear disarmament verification is neutron counting. Such measurements take place in nuclear facilities with concrete rooms. Neutron scattering in building structures can create a significant background, leading to higher measured neutron flux densities as well as a moderated energy distribution. Since neutron measurements may become a major tool in nuclear disarmament verification, assessing the influence of concrete is important for this application. Using Monte Carlo simulations, the impact of concrete building structures on the neutron radiation has been analysed for different scenarios. For a single wall it is shown that for energies between 1 eV and 14 MeV the ratio between reflected and transmitted neutrons depends on the source energy. Moreover, scattering in the concrete causes thermalisation of the neutron energy spectrum. Exchanging regular Portland concrete with radiation protection concrete leads to less reflected and transmitted neutrons, but in the MeV range the difference between the concrete types is small. In a closed room, neutron flux densities depend on the thickness of the walls, the room size, and the concrete composition. In a small room flux densities may be nearly an order of magnitude higher than in an open environment. Different concrete compositions can alter flux densities by a factor of 2 and significantly impact their energy spectra. The effect of the walls can be mitigated by enclosing both measurement sample and detector in a standardised neutron absorbent casing.

Keywords: nuclear disarmament; neutron counting; concrete; neutron scattering

1. Introduction

Despite a reduction of nuclear weapons stockpiles in the past decades, there is still no verification regime enforcing the global irreversible disarmament of nuclear warheads. Since 2015, the International Partnership for Nuclear Disarmament Verification (IPNDV) is developing verification approaches, procedures, and technologies [1].

Disarmament verification procedures include gamma and neutron radiation measurements to confirm the presence or absence of fissile material as well as spectrometric analyses to validate its isotopic composition [2, 3]. The specific measurement techniques (active or passive, count rate or spectrometry) are still under discussion, but it is widely assumed they will include passive neutron counting. In using a method called template measurement a container holding a nuclear warhead can be measured at various different stages of the dismantlement process to ensure its contents have remained unchanged [4] without revealing absolute or relative values of properties that characterize the item. However, if the measurements conducted in different environments were to yield different results for the same item, the template method would falsely indicate the diversion or manipulation of fissile material.

In closed rooms, concrete walls influence measurements by absorbing, moderating, and reflecting neutrons. Corrections for neutron scattering from walls etc. are not readily available but methods were developed e.g. for the calibration of neutron detectors [5]. As the exact shielding characteristics of concrete are highly important for radiation protection, they are widely studied, e.g. for radioactive waste [6] or for spallation sources for which a special concrete with polyethylene and boron carbide has been developed to effectively shield the neutron radiation [7]. Differences in shielding effectiveness [8] and their effect on reactivities of fissile materials [9-11] have been analysed for different concrete compositions, but there is a lack of assessments of their reflection potential.

Neutron reflection by concrete is important in the verification of nuclear disarmament since the reflected neutrons can reach a detector and increase the measured neutron flux. Gregor et al. [12] have shown how the neutron signal of a detector in a closed room deviates from the simplified $1/d^2$ assumption and that this deviation depends on the measurement environment. They concluded that at distances of practical interest greater than 50 cm from the neutron source, the reflected neutrons outnumber the direct neutrons and therefore the calculation of the source activity based on the measured neutron flux densities has to be corrected for this effect. They also demonstrated experimentally the effect of room sizes on measurement results. Analytic expressions [13] as well as Monte Carlo

simulations [14] have shown that for small and intermediate sized rooms reflected neutron flux densities correlate well with room surface areas.

In disarmament verification, measurements on an intact warhead are assumed to take place at a distance of at least 1 m from the warhead [15]. Therefore, the effect of walls on the measured neutron flux densities, which is significant as discussed above, has to be taken into account.

In this paper, a systematic analysis of the impact of concrete building structures on neutron radiation will be presented based on Monte Carlo simulations of neutron transport. It includes a neutron beam directed at a single wall as well as neutron flux densities of an intact warhead modelled after the Fetter design [16] in a closed concrete room. The impact of the concrete composition is analysed for ordinary concrete as well as radiation protection concrete. The thickness of the building structures in nuclear weapons facilities may be unknown or undisclosed. Therefore, a series of simulations were performed varying the thickness of the concrete structures. Finally, the effect of room size was analysed.

2. Materials and Methods

In this study, Monte Carlo simulations were performed, as these allow varying concrete composition, density, and changes in its hydrogen concentration due to varying humidity [10]. Gregor et al. have shown that Monte Carlo simulation can well reproduce neutron measurements in concrete rooms [12]. We used the open-source simulation toolkit Geant4, which has been developed at CERN, the European Organization for Nuclear Research, and is used in various applications including high energy physics as well as medical science [17]. The ENDF/B-VIII.0 cross section library [18] was used. Fission processes were simulated with the G4ParticleHPFission model. The applicability of our code has been validated using plutonium-uranium mixed oxide configurations of various masses, shieldings (bare, cadmium, lead, high-density polyethylene), and concentrations as well as isotopic compositions of the plutonium [19].

Ordinary concrete like Portland concrete and radiation protection concrete with additives such as boron and barium were investigated. A range of concrete compositions are specified in Table 1.

The thickness of walls in nuclear facilities is generally not disclosed for security reasons. A value of 20 cm was chosen as a reasonable default wall thickness which was then systematically varied to quantify the effect on the simulated neutron scattering.

Element	Mass fraction [%]		
	Portland	Baryte	Boron carbide
Hydrogen	1.00	0.36	0.36
Boron	–	–	61.55
Carbon	0.10	–	17.16
Oxygen	52.91	31.16	9.58
Fluorine	–	–	–
Sodium	1.60	–	–
Magnesium	0.20	0.12	0.12
Aluminium	3.39	0.42	0.42
Silicon	33.70	1.05	1.05
Sulphur	–	10.79	–
Potassium	1.30	–	–
Calcium	4.40	5.02	5.02
Manganese	–	–	–
Iron	1.40	4.75	4.75
Zinc	–	–	–
Barium	–	46.34	–
Density [g/cm ³]	2.30	3.35	2.30

Table 1: Composition of the different types of concrete. The Portland and Baryte concrete specifications are taken from McConn Jr. et al. [20], the Boron carbide concrete composition is the authors' own estimate whereby the structural properties have not been checked to be suitable for walls. Nevertheless, it gives a good impression of the effect of a high boron amount in concrete.

As neutron source for our calculations, the notional warhead model developed by Fetter et al. [16] was adopted. It consists of a hollow sphere of 4 kg of weapon-grade plutonium surrounded by a beryllium reflector, an uranium tamper, high explosives (such as triaminotrinitrobenzene [21]) and an aluminium casing. For security and safety reasons, the warhead is placed in a steel container with a Celotex lining (Fig. 1), a lignocellulosic fibreboard whose chemical composition can be approximated by cellulose [20]. The plutonium has a primary neutron source strength of approximately 190 kBq due to spontaneous fission of Pu-240. The energy distribution of the neutrons emitted by the plutonium was modelled as a Watt spectrum

$$X(E) = \exp\left(\frac{-E}{a}\right) \cdot \sinh(\sqrt{b \cdot E})$$

with the Watt parameters $a = 0.7949$ MeV and $b = 4.689$ MeV⁻¹ [22].

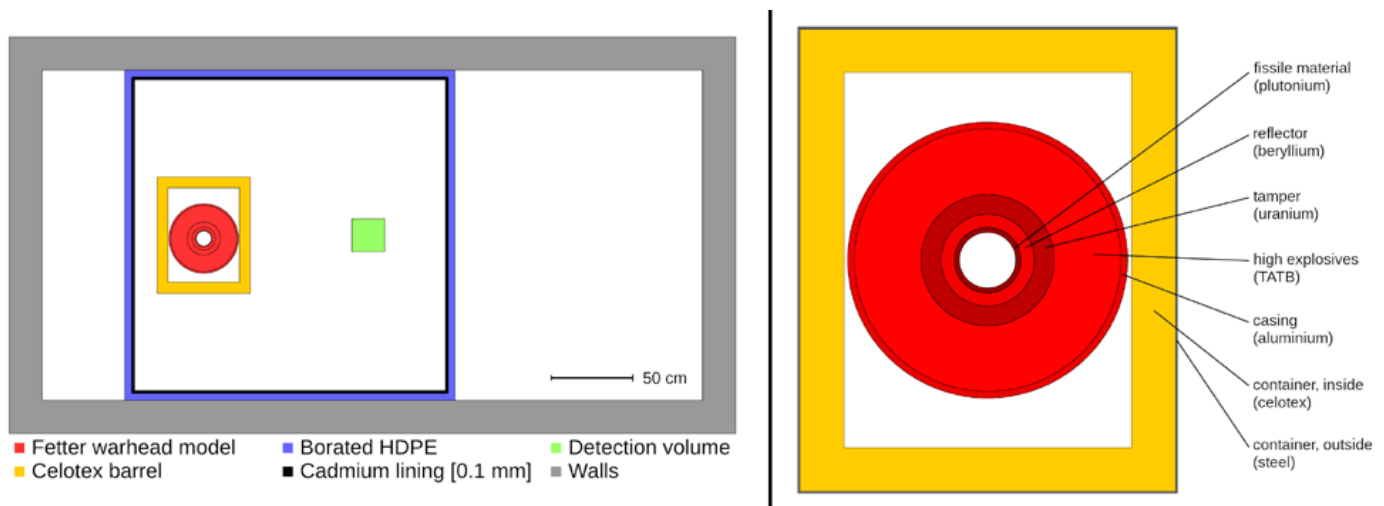


Figure 1: Side view cut (left) of the simulated standard geometry. A nuclear warhead, as modelled by Fetter [16], (right) is placed in a Celotex container in a 4 m by 3 m by 2 m room. Neutron flux densities are counted in the detection volume. For the simulation presented in Section 4, a 2 m by 2 m by 2 m neutron shielding box containing borated high-density polyethylene was placed around source and detection volume in order to mitigate neutron back scattering from the walls.

Two scenarios were studied: I. A neutron beam directed at a concrete wall and II. A nuclear warhead positioned in a closed room with concrete walls.

Scenario I:

To systematically study the impact of concrete walls on neutrons, a beam directed at a single wall was simulated. A monoenergetic point source was emitting neutrons towards the centre of a 4 m by 4 m concrete wall. In the simulation, neutron energies were varied between 1 eV and 14 MeV. Reflected as well as transmitted neutrons were counted, and their energy spectra recorded.

In addition, the effect of reinforced concrete was studied by assuming a lattice of 2 cm diameter high carbon steel [20] bars present at the centre of the wall. They were placed at 10 cm intervals in both directions.

Scenario II:

During nuclear dismantlement verification inspections, measurements will presumably be performed in closed rooms. The background will include not only neutrons scattered back from air, walls, floor and ceiling, but also neutrons eventually entering the detector after multiple scattering events in the room structure. A simplified scenario of such a measurement setup has been analysed.

A reference room with a floor area of 4 m by 3 m and a height of 2 m was modelled. Its floor, ceiling and walls are assumed to consist of 20 cm thick Portland concrete. A notional nuclear warhead with a primary neutron activity by spontaneous fission of Pu-240 of 190 kBq (secondary neutrons are produced by induced fission in Pu with a neutron activity of 360 kBq and by neutron interaction processes in the reflector and tamper of 162 kBq) according to Fetter et

al. [16] is situated in a steel container with a 6.6 cm thick Celotex lining. The container is placed 1 m away from the centre of the room. The warhead model has a radius of 21 cm, its container a radius of 28.5 cm and a height of 71 cm.

The room geometry was varied by successively shifting the walls outward in steps of 1 m, thereby enlarging the room from 4 m by 3 m to 24 m by 23 m. For each size, simulations were repeated for three different heights of the ceiling (2, 4 and 6 m).

Instead of simulating a specific detector, the neutron flux densities in a 20 cm by 20 cm by 20 cm sampling volume made of air located at the centre of the room were simulated and recorded. Positioning the detector 1 m from the warhead container is a reasonable assumption for an inspection [15].

3. Results and discussion

3.1 Neutron beam directed at a single wall

The fractions of neutrons which are reflected, absorbed, or transmitted by a 20 cm wall of the concrete types studied are given in Figure 2. Some general trends become apparent. First, there are only slight differences between Portland and Baryte concrete despite their different composition. In contrast, neutrons with source energies of 1 MeV and lower show high absorption rates in boron carbide concrete. This effect becomes more pronounced for lower source energies, which closely reflects the energy dependence of the boron absorption cross section. Second, for neutrons with source energies typical for a fission spectrum (exceeding 1 MeV) the reflected fraction decreases about 50 % compared to source energies of 1 MeV or lower for all three

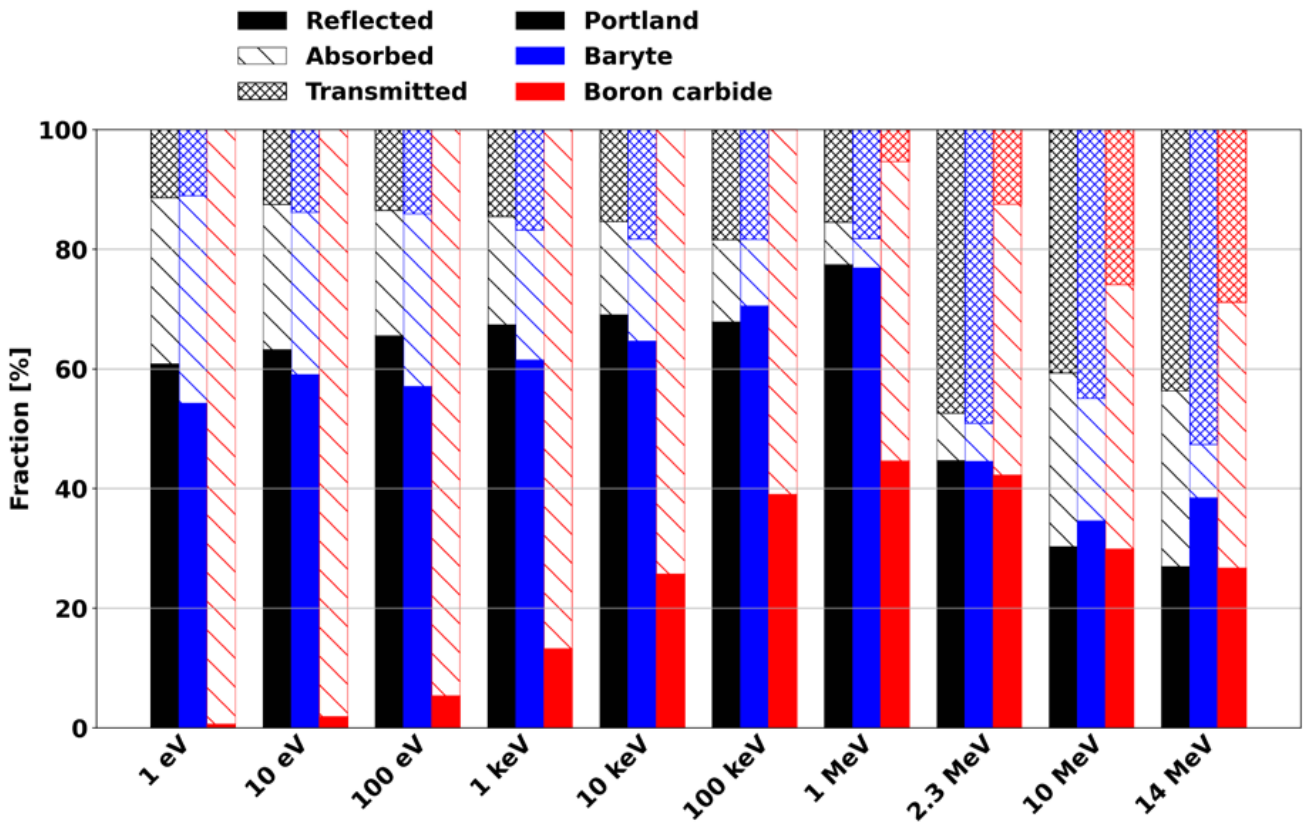


Figure 2: Fractions of reflected, transmitted and absorbed neutrons for a 20 cm concrete wall, by source energy and concrete type.

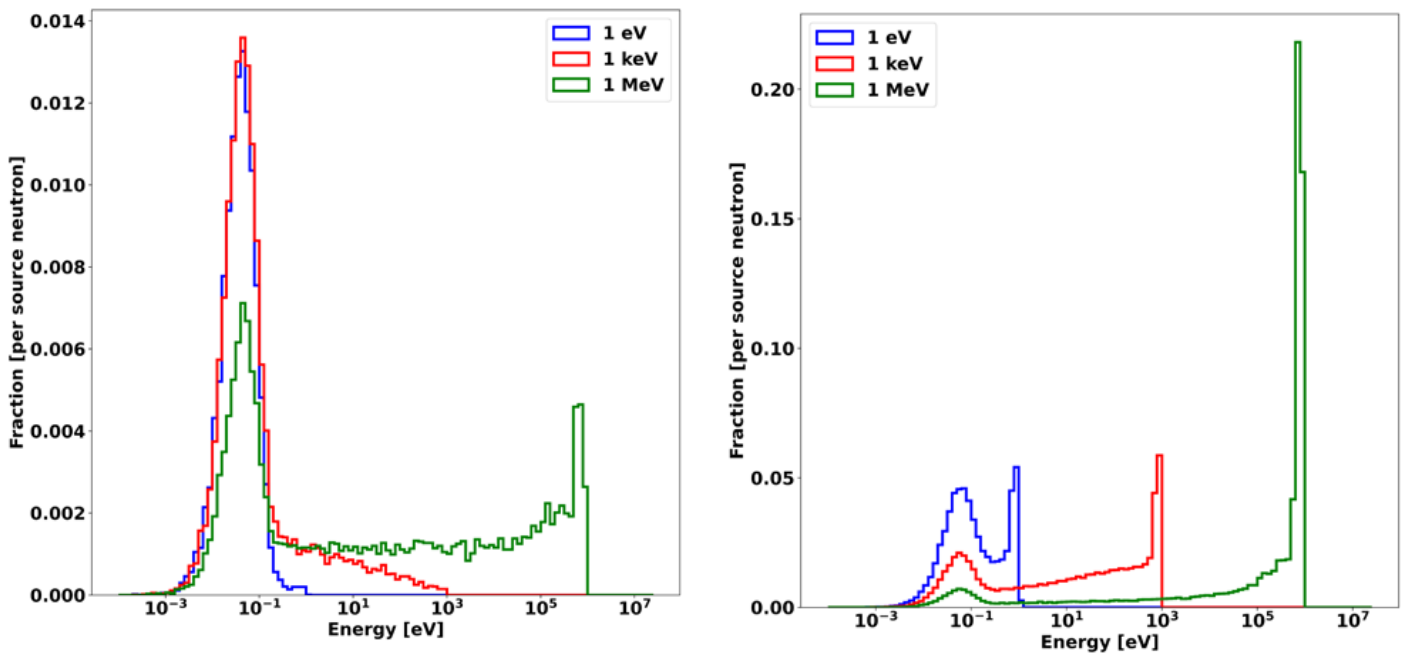


Figure 3: Energy distributions of transmitted (left) and reflected (right) neutrons by a Portland concrete wall for three different source energies.

concrete types. Again, the boron carbide concrete shows an elevated absorption rate due to neutron moderation within the concrete and absorption by ^{10}B .

If reinforced with steel rebar (results not shown), the fractions of reflected neutrons are slightly higher for all three concrete types (< 5 %). The transmitted fractions are slightly affected by additional absorptions of moderated neutrons by the steel.

These results confirm and extend previous analyses on the reflection of neutrons by concrete building structures [8, 12–14]. This reflection is even present if building structures consist of boron carbide concrete intended for effective neutron shielding, although neutron background levels are considerably reduced compared to ordinary Portland or high-density gamma shielding Baryte concrete

For the common Portland concrete, energy spectra of reflected and transmitted neutrons are shown in Figure 3 for three different source energies. For the transmitted neutrons (Fig. 3, left), the moderating effect of the concrete becomes obvious: at source energies of 1 eV and 1 keV transmitted neutrons are almost thermalised, but even 44% of the transmitted 1 MeV neutrons display energies < 1 eV after transmission. The energy distributions of the reflected neutrons (Fig. 3, right) demonstrate the small scattering cross section of fast neutrons compared to epithermal and thermal source energies.

The reinforced concretes (results not shown) do not show significantly different energy distributions of reflected neutrons, but a slightly smaller thermal peak of transmitted neutrons due to the higher absorption of low energy neutrons in the steel. Since the presence of rebar does not have a major impact and information on the design of the concrete structures in nuclear weapons handling facilities is expected to be confidential, the results presented in the following are for pure concretes.

3.2 Nuclear warhead in a closed room

In the following, the flux densities and energy distributions of neutrons emitted from the notional warhead model entering the detection volume in the closed concrete room are analysed. Results are shown in Table 2 and Fig. 4 for room structures with concrete walls of 20 cm thickness. For comparison, results are included for the hypothetical case that no surrounding structures are present to indicate the direct neutron flux. For the common Portland, but also for Baryte concrete, reflected neutrons dominate flux densities at the detection volume, but even for the neutron shielding B_4C concrete reflected neutrons contribute about 33% to the recorded signal. As was shown in Fig. 3 above, both Portland and Baryte concrete effectively moderate the reflected neutrons. Differences in peak heights at thermal energies are caused by the higher hydrogen content of the Portland concrete (compare Table 1). Thermalisation is not

visible for boron carbide concrete structures due to the strong absorption of scattered neutrons with energies below 100 eV. Fig. 4 shows that even without any background of reflected neutrons, the emitted spectrum is moderated. This effect is caused by the high explosives of the warhead.

concrete type	flux density [$\text{cm}^{-2} \text{s}^{-1}$]	flux density in absorption box [$\text{cm}^{-2} \text{s}^{-1}$]
none	2.14 ± 0.03	3.20 ± 0.04
Portland	5.71 ± 0.05	3.25 ± 0.04
Baryte	4.82 ± 0.05	3.32 ± 0.04
Boron carbide	2.84 ± 0.04	3.26 ± 0.04

Table 2: Neutron flux densities in the detection volume for different concrete types of the building materials. The second column shows the flux densities when source and detection volume are enclosed in a neutron absorbent box made from borated polyethylene and cadmium.

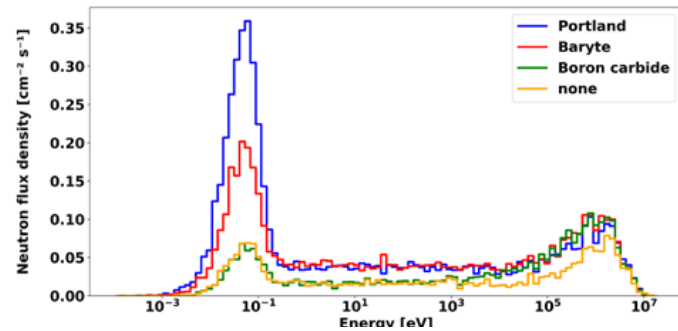


Figure 4: Energy distributions of neutrons inside the detection volume in the reference concrete room for various types of concrete; for comparison, a spectrum without any reflecting structures outside the nuclear warhead is shown.

3.3 Thickness of building structures

The simulation results shown in Fig. 5 show that due to reflection in the Portland concrete neutron flux densities in the room rise quickly when increasing the thickness of the walls (including floor and ceiling), converging already at approximately 20 cm. The physical reason for this convergence is the penetration depth of the reflected neutrons (Fig. 6): the vast majority of the reflected neutrons do not penetrate the concrete more than 15–20 cm. Since it is reasonable to assume that walls in nuclear weapon maintenance and storage facilities commonly will exceed this value, the simulations presented here for a default thickness of 20 cm can be generalized.

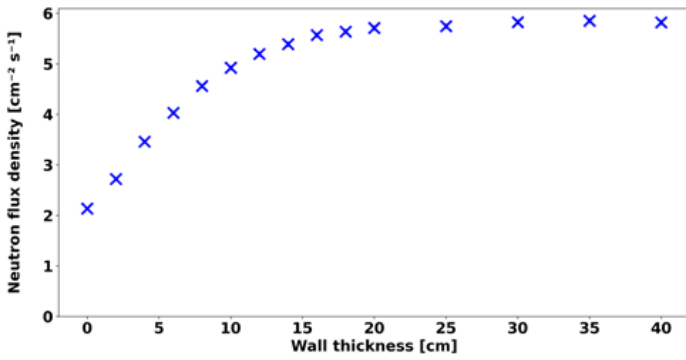


Figure 5: Calculated neutron flux densities in the detection volume as a function of building structure thickness for the notional Fetter nuclear warhead model.

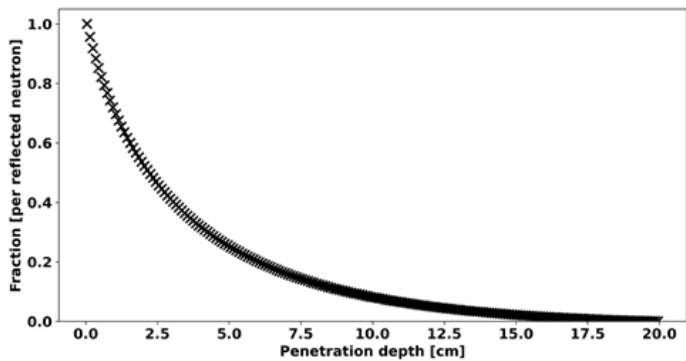


Figure 6: Penetration depth of neutrons before they are reflected back into the reference room. Each bin shows the cumulative fraction of neutrons reaching the designated depth. Absorbed and transmitted neutrons are not counted.

3.4 Room size

Simulated neutron flux densities within the modelled detector volume for varying room sizes are shown in Fig. 7. The value without any surrounding structures is given as reference. When enlarging the room area, the calculated neutron flux densities become smaller until they converge when the wall shift reaches 4 m, corresponding to a room size of 12 m by 11 m. At this point, the converged flux density is still larger than without concrete building structures as the floor is still present. A corresponding effect is observed when increasing height of the room until the neutron flux converges at about 4 m. However, for all room sizes the contribution of scattered neutrons to the total flux density remains significant and a small room may increase it by a factor of 2 compared to a large room.

4. Mitigating the impact of concrete structures

Due to the high price of boron carbide concrete, which is around 3300 times that of Portland concrete [23], routine operations (nuclear warhead maintenance, dismantlement, storage, and verification measurements) will most likely be performed in ordinary concrete buildings with high neutron reflection potential. For nuclear disarmament verification promising analytical technologies include neutron template

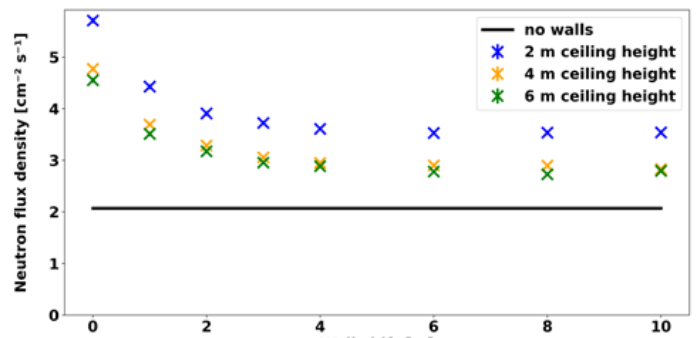


Figure 7: Neutron flux densities for the notional nuclear warhead in the modelled detector volume as a function of room area and ceiling height. The simulated room size starts out at 3 m by 4 m and is successively increased by shifting all walls outward. The straight line shows the flux density without any reflected neutrons.

measurements [4] and imaging [24]. Depending on the concrete and on the position of source and detector relative to the building walls reflected neutrons may dominate the neutron signals and invalidate such analyses.

Thus, a strategy to mitigate the influence of concrete structures on measured neutron signals is proposed. Inspired by the Pulsed Neutron Interrogation Test Facility (PUNITA) at the Joint Research Center of the European Commission [25], it is suggested to place sample and detector inside a box, which is designed (i) to minimise neutron flux densities leaving the box and therefore backscattering and, (ii) to reduce reflected neutron fluxes before entering the box' interior. This is achieved by using materials with high neutron moderation and absorption potentials [26]. In the following the effect of a cubic box of 2 m by 2 m by 2 m is analysed, which allows keeping a suitable distance between warhead container and detector. Walls, bottom and top of the container are made from 5 cm borated (35 %) high-density polyethylene slabs. An inner lining of 0.01 cm cadmium foil is included to absorb thermal neutrons and minimise backscattering of moderated neutrons into the detector volume. It was confirmed (data not shown) that increasing the thickness of the polyethylene shields did not have a significant effect on the neutrons flux inside the box.

The simulation results in Table 2 show that when using this measurement box, the recorded neutron flux densities are nearly identical for all concrete types and even for the hypothetical scenario that no neutron reflecting material is present outside the box. Comparison with the corresponding flux densities without the shielding box indicate that about 30% of the neutrons reaching the detector volume are backscattered by the polyethylene box itself. As expected, this results in shifting the energy distribution of the neutrons in the detector volume to lower energies, but without masking the spectrum of the neutrons emitted by the warhead (Fig. 8).

These results demonstrate that by using a shielding box as described the influence of concrete building structures on the neutron flux densities can be eliminated while keeping its own moderating effect of the neutrons at a tolerable level.

Using such boxes hence allows to apply almost all neutron verification technologies at each position during the nuclear disarmament process (deployment area, interim and long-term storage, dismantlement facility) without being affected by concrete walls, although their sizes may need to be adjusted for some measurement technologies. A significant neutron activation of their materials is not to be expected, since the materials of the proposed box are identical with those of neutron coincidence counters used in safeguards. It can be expected that each facility used for this process will have some area which will be dedicated to verification activities including potential gamma and neutron measurements. Each of these could be provided with such a shielding box for neutron verification analyses under standardised conditions. These may include template measurements – both of total fluxes and of energy distributions with e.g. a Bonner sphere type detector [27] for verification of the presence of high explosives in an assembled warhead – as well as imaging analyses [24]. Since the number of dismantlement facilities will be limited in each nuclear weapon state, the effort for installing the boxes will be low despite their weight and lack of mobility.

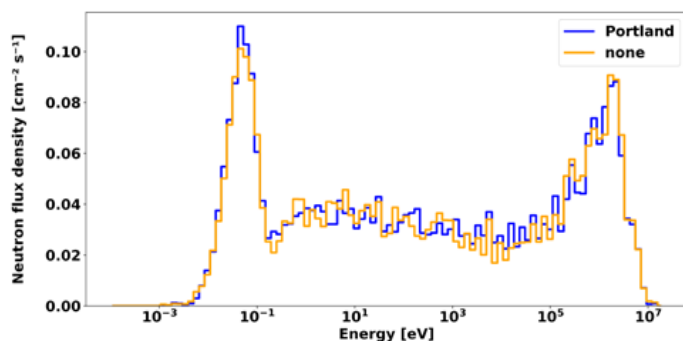


Figure 8: Spectra of the neutrons inside the sampling volume when neutron source and sampling volume are situated within a neutron absorption box consisting of polyethylene and cadmium.

5. Conclusions

The results presented in this study contribute to the knowledge on flux densities and energy distributions of neutrons reflected and transmitted by concrete building structures. These effects are quantified as functions of concrete types, including a highly borated concrete, room size and thickness of the concrete structures.

For its application in the context of nuclear disarmament verification, neutron measurement results should ideally be independent of sample positioning and the surrounding building structures, in particular for neutron imaging and

template measurements, which rely on the reproducibility of neutron flux densities and their energy distributions. This problem can be solved by conducting the measurement in a neutron absorbent casing, constructed from borated polyethylene and an inner cadmium liner. Calculations show that such a casing has the potential to mitigate the influence of neutron reflection from the surrounding walls while introducing only a moderate and reproducible background of neutrons backscattered by the casing. Installing such a box in those facilities of the nuclear weapons complex which will be dedicated to disarmament verification activities will contribute to flexible and versatile nuclear disarmament verification strategies and to the confidence they will achieve.

6. References

- [1] Hinderstein C; International Partnership for Nuclear Disarmament Verification: Laying a foundation for future arms reductions; Bulletin of Atomic Scientist; vol. 74; 2018; pp. 305-311; see also <https://www.ipndv.org>, accessed August 2022.
- [2] Runkle RC, Bernstein A, Vanier PE; Securing special nuclear material: Recent advances in neutron detection and their role in nonproliferation; Journal of Applied Physics; vol. 108; 2010; 111101.
- [3] Göttsche M, Kirchner G; Measurement Techniques for Warhead Authentication with Attributes: Advantages and Limitations; Science & Global Security; vol. 22; 2014; pp. 83-110.
- [4] Yan J, Glaser A; Nuclear Warhead Verification: A Review of Attribute and Template Systems; Science & Global Security; vol. 23; 2015; pp. 157-170.
- [5] Kim SI et al.; A review of neutron scattering correction for the calibration of neutron survey meters using the shadow cone method; Nuclear Engineering and Technology; vol. 47; 2015; pp. 939-944.
- [6] Jallu F, Passard C, Brackx E; Application of active and passive neutron nondestructive assay methods to concrete radioactive waste drums; Nuclear Instruments and Methods in Physics Research B; vol. 269; no. 18; 2011; pp. 1956-1962.
- [7] DiJulio DD et al; A polyethylene-B4C based concrete for enhanced neutron shielding at neutron research facilities; Nuclear Instruments and Methods in Physics Research A; vol. 859; 2017; pp. 41-46.
- [8] Piotrowski T; Neutron shielding evaluation of concretes and mortars: A review; Construction and Building Materials; vol. 277; 2021; 122238.
- [9] Handley GR, Robinson RC, Cline JC; Effects of Concrete Composition in Nuclear Criticality Calculations; Transactions of the American Nuclear Society; vol. 61; 1880; pp. 182-184.

- [10] Wetzel LL; Amount and Effect of Moisture Retention in Concrete; Data Analysis for Nuclear Criticality Safety; vol. 63; 1991; pp.217-218.
- [11] Monahan SP; The Neutron Physics of Concrete Reflectors; Fifth International Conference on Nuclear Criticality Safety; Albuquerque; 17 – 21 September 1995; LA-UR-95-2196; Revised; LA-UR-07-5898; 2007; https://mcnp.lanl.gov/pdf_files/la-ur-07-5898.pdf (accessed October 12, 2022).
- [12] Gregor J, Baron M, Kesten J, Kroeger EA; Comparison of the response of handheld neutron detectors in differing deployment environments: Measurements, calculations and practical implications; Radiation Measurements; vol. 143; 2021; 106571.
- [13] Eisenhauer CM, Hunt JB, Schwarz RB; Calibration Techniques of Neutron Personal Dosimetry; Radiation Protection Dosimetry; vol. 10; 1985; pp. 43-57.
- [14] Khabaz R; Analysis of neutron scattering components inside a room with concrete walls; Applied Radiation and Isotopes; vol. 95; 2015; pp. 1-7.
- [15] Oral communication by representatives of nuclear weapon states during IPNDV meetings.
- [16] Fetter S et al.; Detecting Nuclear Warheads; Science & Global Security; vol. 1; 1990; pp. 225-263.
- [17] Allison J et al.; Geant4 developments and applications; IEEE Transactions on Nuclear Science; vol. 53; 2006; pp. 270-278.
- [18] Brown DA et al.; ENDF/B-VIII.0: The 8th Major Release of the Nuclear Reaction Data Library with CIELO-project Cross Sections, New Standards and Thermal Scattering Data; Nuclear Data Sheets; vol. 148; February 2018; pp. 1-142.
- [19] Kreutle M, Borella A, Rossa R, Scholten C, Kirchner G, van der Meer C; Benchmarking Monte Carlo Simulations in the context of nuclear disarmament verification via Monte Carlo simulations with GEANT4; INMM & ESARDA Joint Virtual Annual Meeting; 23. - 26. 8. & 30. 8. - 1. 9. 2021.
- [20] McConn Jr. RJ, Gesh CJ, Pagh RT, Rucker RA, Williams III RG; Compendium of Material Composition Data for Radiation Transport Modelling; Pacific West Laboratory; 2011.
- [21] Withworth NJ; Modelling detonation in ultrafine TATB hemispherical boosters using CREST; Conference "Shock Compression of Condensed Matter – 2011"; Chicago; 26 June – 1 July 2011; American Institute of Physics Conference Proceedings 1426 (2012); pp. 213-216.
- [22] Shores E; Data updates for the SOURCES-4A computer code; Nuclear Instruments and Methods in Physics Research B; vol. 179; no. 2; 2001; pp. 78-82.
- [23] Federal German Association of the Cement Industry; Heavy Concrete / Radiation Protection Concrete; Cement Data Sheet Concrete Technology B 10; 2002 (in German).
- [24] Brennan J et al.; Demonstration of two-dimensional time-encoded imaging of fast neutrons; Nuclear Instruments and Methods in Physics Research A; vol. 802; 2015; pp. 76-81.
- [25] Favalli A, Mehner H-C, Crochemore, J-M, Pedersen B; Pulsed Neutron Facility for Research in Illicit Trafficking and Nuclear Safeguards; IEEE Transactions on Nuclear Science; vol. 56; 2009; pp. 1292-1296.
- [26] Stone MB; Crow L; Fanelli VR; Niedziela JL; Characterization of shielding materials used in neutron scattering instrumentation; Nuclear Instruments and Methods in Physics Research A; vol. 946; 2019; 162708.
- [27] Dubeau J, Hakmana Witharana SS, Atanackovic J, Yonkeu A, Archambault JP; A Neutron Spectrometer Using Nested Moderators; Radiation Protection Dosimetry; vol. 150; 2012; pp. 217-222.

Integration of independent NDA techniques within a SLAM-based robotic system for improving safeguards standard routines: a review of the current status and possible future developments

Filippo Gagliardi

Nucleco spa, Radiological Characterization Plants Section, Via Anguillarese 301, Rome 00123 (RM), Italy
La Sapienza – University of Rome, DIAEE – Department of Astronautical, Electrical and Energy Engineering
Corso Vittorio Emanuele II 244, Rome 00186 (RM), Italy

E-mail: gagliardi@nucleco.it

Abstract:

Agencies devoted to safeguard and non-proliferation make large use of techniques based upon non-destructive assays (NDA) systems for ensuring the correctness of operator declarations about a facility inventory or for gathering data during inspections. The data ensemble to analyse consists of many aspects, but it is mainly focused on radiological data. De facto, systems used for NDA radiological characterization are optimized for precise goals in order to maximize their efficiency and ease of use, at the expense of versatility and more complete (although complex) results. Nevertheless, this approach may encounter several limitations due to the intrinsic properties of the techniques involved. For example, proper background estimation and subtraction in a gamma spectrometry are not always possible, either due to photons mean free path in matter or to the possible inability to suppress external contributions by placing the detector close to the item in object.

A Concept of a modular, multi-sensor system is presented, where the results of radiological and non-radiological assays are automatically integrated in a 3-dimensional model created by means of novel results in robotics and optical sensors. This review paper reports and discuss the state-of-art in the implementation of systems similar to the Concept presented, as the idea behind the Concept has already been tested in recent years with promising results; nevertheless, technology develops fast in the field and new future implementations, improvements and applications in safeguards and non-proliferation are worth to be envisaged, presented and discussed. For example, some of the Concept sensors can also be used as a stand-alone detector, with a natural gaining in the Concept versatility: a high-resolution gamma spectrometer can be used to measure Plutonium isotopic composition or Uranium enrichment. Moreover, results obtainable through the Concept can be used to create a digital twin of a generic component, system, or facility, complete with several radiological and non-radiological data, resulting in a dramatic step forward in the implementation of the Building Information Modelling (BIM) standards.

Keywords: safeguards, non-proliferation, SLAM, gamma imaging, BIM.

1. Introduction

Within the scope of safeguards and non-proliferation of Special Nuclear Materials (SNM), several tasks are accomplished by legally authorized agencies (e.g., the International Atomic Energy Agency, IAEA), including Design Information Verification (DIV), consistency checks on nuclear material accountancy, independent on-site inspections and unattended containment and surveillance (C/S).

Inspection of complex equipment and facilities processing or storing nuclear materials can be a very cumbersome process. For example, a change in the original facility design can suggest that its original purpose was altered, which can suggest malicious proliferating intentions. Visual inspection is not always a reliable way to identify changes in the facility design, but in last years it has been supported by 3-dimensional reconstruction methods like the 3D DIV, a way to create a time-trackable 3-dimensional map of a generic site by means of devices like Laser Scanners or LIDARs (LIght Detection And Ranging) [1]. Moreover, similar optical techniques are used to ascertain seals' integrity.

Periodical inspections, on the other side, usually rely on independent radiological characterization measurements, by means of Non-Destructive Assay (NDA) or Destructive Assay (DA) depending upon the goal of the campaign. NDA characterization is performed in-situ using systems both available off-the-shelf (COT) or specifically tailored to reach precise goals, like quantifying Uranium enrichment, establishing Plutonium isotopic composition or estimating the fuel burn-up through fissile products. Depending upon the measurements' scope, the systems used are equipped with detectors, electronics and software with characteristics developed to optimize the assay. In this sense, efficiency and ease of use are often preferred respect to versatility (which often hides complexity). Nevertheless, standard safeguards routine using non-destructive assays may face several limitations, like the impossibility/inability to get close

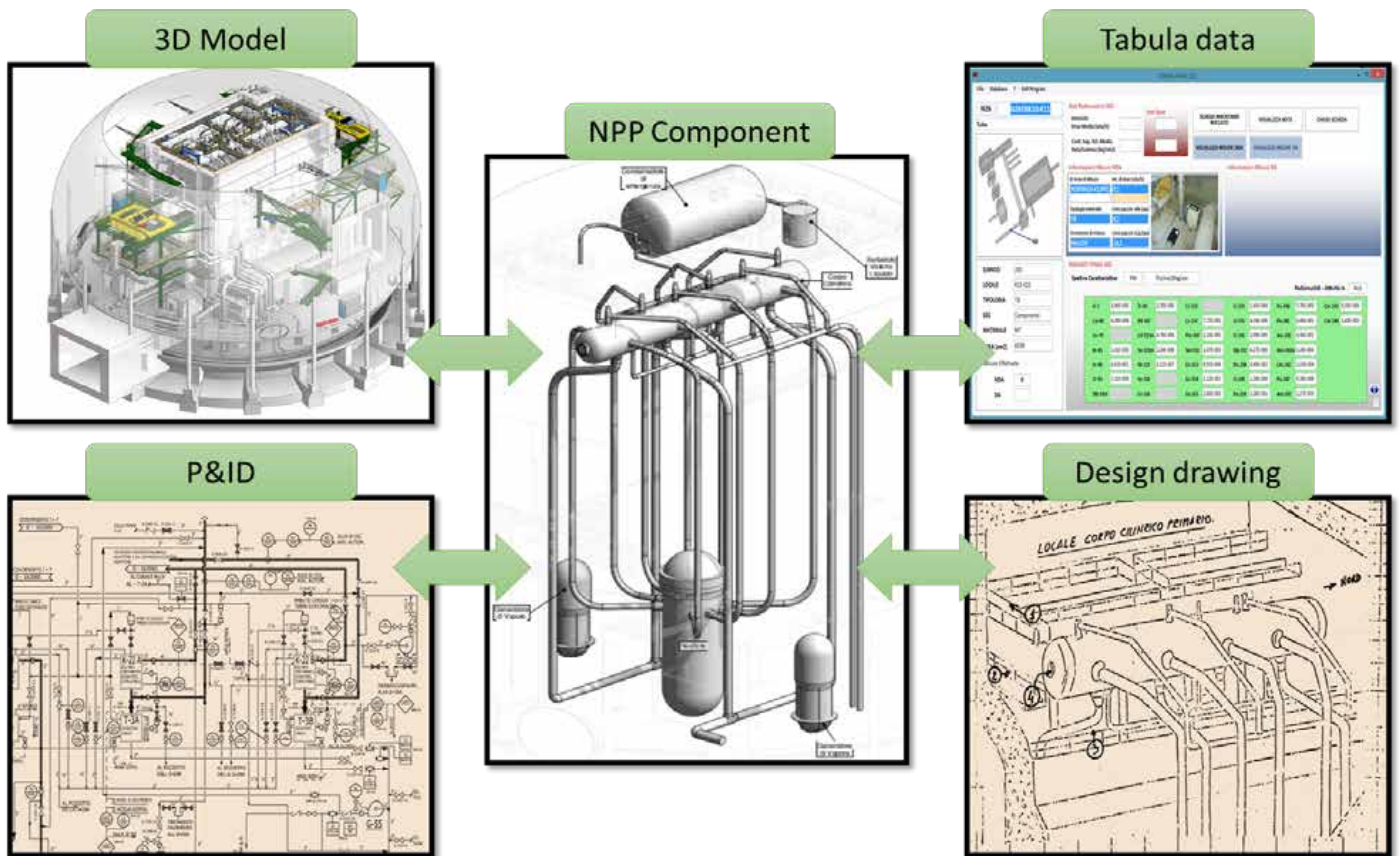


Figure 1: Example of application of K-PIM principles in a real-life NPP. Courtesy of Nucleco spa.

enough to the inspected item (because of processing items hindering the access), the omni-directionality of gamma detectors (despite eventual small shields and collimators used) and the workforce and time needed to survey a complete area/facility.

About surveillance, the need to ensure the Continuity of Knowledge (CoK) between sequential inspections is usually achieved by means of optical cameras, radiological monitors (like gamma detector and neutron counters) and other sensors (e.g., weighing devices, tank level sensors, identity reader). All these devices collect and store a continuous flow of measurements, for which adequate analysis and data interpretation is needed in order to be able to describe the (current) status of the facility they are installed in.

The goal is to obtain a model from which physical and radiological information can be retrieved and whose data is automatically integrated in the digital twin in a way it can be both visualized and quantitatively used for safeguard's goals. From a non-proliferation perspective, the possibility to combine different techniques and using multiple sensors (stand-alone or as a unique integrated device) would optimize the effort required and increase safeguard effectiveness. From the management perspective, the possibility to have a tool for creating a digital twin of the facility might dramatically improve its monitoring and future

decommissioning according to the Building Information Modelling (BIM) standards.

The structure of this manuscript is as follow. Firstly, this paper introduces the possibility to use different techniques (novel techniques or techniques using technology either off-the-shelf or known to be under development) in order to create a 3-dimensional digital twin of a generic facility (with all the components within it). Then, the paper reviews the state-of-art of systems similar to the Concept, highlighting the gaps still to be filled for its future mature application in safeguards and non-proliferation.

2. The Concept: techniques and technologies involved

The goal of the proposed Concept is to (semi)automatically create a time-tracked 3D model of a certain facility including radiological information and multiple sensors data. As such, the data ensemble and the tool for visualization and data management (through a common database usually called Common Data Environment, CDE) are a direct application of BIM standard through the Knowledge-centric Plant Information Modelling (K-PIM) principles as suggested

by IAEA [2] (see Figure 1). The principle of integrating different information in a model (i.e., a scene) is known as Scene Data Fusion (SDF) [3].

The Concept would consist of (at least):

- **SLAM Architecture** - The Simultaneous Localization And Mapping (aka SLAM [4]) engine represents the core of the Concept. This engine is needed to create the 3D model of the area of interest with its coordinate system and to determine the sensors' position within it.
- **Radiation sensors** – Data from those sensors can be included directly in the 3D model (but this requires the results to be fit for such visualization) or can fill a database created from the 3D model.
- **Non radiation sensors** – Thanks to the 3D model created by the SLAM architecture and to its capability to process the system position inside the map, many possible sensors might be introduced, as long as their output can be related to the sensor's position (known by SLAM) or can be applied to part of the 3D model. These sensors will not be discussed in this paper.

2.1 SLAM Architecture

As already mentioned, the Simultaneous Localization And Mapping (SLAM) engine represents the core of the Concept. This engine's task is to create a point cloud of a certain area or facility (example in Figure 2). The point cloud is

used as a 3-dimensional representation of the area at a certain time; as such, it (and its coordinate system) can be used to spatially localize any radiological and non-radiological information that can be visualized directly on the point cloud or in an automatically built database. In the rest of this paper the Concept of point cloud and 3D model will be used as synonyms, while a clear distinction will be made when talking about parametric 3D model (like the ones created using CAD or similar tools).

The minimum hardware needed for running the SLAM engine is:

- *Sensors for point cloud acquisition*, typically a LIDAR (acquiring the point cloud with a certain frequency) coupled with an odometry camera (for determining position and pose – aka orientation – of the device inside the space). The creation of the complete facility's point cloud is performed merging all the LIDAR-acquired point clouds, guessing information about LIDAR position and pose in the space using the odometry camera and then performing a global optimization process as long as new point clouds are acquired. In order to properly complete the map, the LIDAR needs to be moved inside the space. Example of SLAM engine are Cartographer [5], RTAB-Map [6] or ORB-SLAM3 [7].

- Point clouds can be acquired also using other devices, like laser scanners (a sort of static version of LIDAR) or using optical camera with Time-of-Flight



Figure 2: Point cloud of a Boiling Water Reactor building. Courtesy of Nucleco spa.

sensor. Changing sensors imply adapting algorithms and obtaining results with different complexity and detail level, as long as a different effort required for data acquisition and constraint to be respected. Although LIDAR are mostly used in the first system developed worldwide, at the end of the day the choice of the sensors is something that as to be performed depending upon the goal desired.

- *An on-board computational unit* able to run a dedicated operating system (a ROS – Robotic Operating System) and with enough power and storage to manage sensors data, in particular merging the point clouds acquired by LIDAR.

Regardless of the technologies used, it is important to underline that in the last years the creation of 3D model *as-built* by means of point clouds is becoming increasingly accessible, reliable, and mature thanks to the improvement in the computation power and to the possibility of using augmented reality software on common-life tools, like smartphones and tablets. Moreover, in last years the growth of computational power (e.g. parallel CPU/GPU elaboration, quantum computing), the interpretation of point cloud for object identification (and thus for automatic creation of 3D parametric models) is gaining interest in the field of Machine Learning [8] [9].

2.2 Radiation sensors

The presence of a radiation sensors package is the main feature that makes the Concept useful for safeguards and non-proliferation purposes. The underlining idea is to use versatile detectors and techniques, possibly providing outputs that can be represented and visualized. The list of the appropriate radiological sensors includes (but is not limited to):

- Gamma imaging system – The most versatile and reliable technique for this purpose nowadays. Gamma imagers, also called gamma cameras, are able to reconstruct the direction from which the recorded photons are coming. The results can be visualized directly on the point cloud, while the merging within a parametric 3D model is still to be developed.
- Neutron imaging system - This technique is less developed than gamma imaging, but the possible outcomes of its further development might be useful for safeguards and non-proliferation than this possibility needs to be discussed. The results can be visualized directly on the 3D model.
- Dose rate meter – Dose rate can be measured by dedicated sensors or by means of the detectors used for imaging. The visualization is not trivial, but the results could be included in the 3D model as a “hidden” information such as a scalar field and used to evaluate the

total dose absorbed by an operator to accomplish a certain task.

- Other radiological sensors – Possible examples are the continuous air monitors. The results can be integrated into the database as part of the radiation monitoring systems. The 3D model can be used to localize the acquired data.

The world of gamma imaging systems has rapidly grown in the last decades thanks to the improvements achieved in crystals manufacturing, electronics, and algorithms. Different systems exist on the market (or as prototypes) with different characteristics, thus choosing the one to use is a decision to be made depending upon the situation [10] [11] [12] [13] [14] [15] [16] [17] [18]. However, the most mature (and probably versatile) setup sees the usage of a CdZnTe crystal (whose active volume usually ranges from 1 cm³ up to some tens of cm³) with segmented electronics for signal readout, using the Compton Algorithm and/or the Coded Aperture Mask algorithm for imaging reconstruction. In general, CdZnTe crystals are less efficient than NaI(Tl) and have a worse energy resolution than HPGe; nevertheless recent improvements make them much more similar to HPGe in terms of efficiency (higher crystals are possible thanks to a better management of the crystal impurity) and energy resolution (less impurity means also a better charge collection in the crystal, thus a better resolution), with the crucial advantages of being able to work at room temperature (without the HPGe annoying need to be cooled) and to permit an easy way to apply segmented electronics.

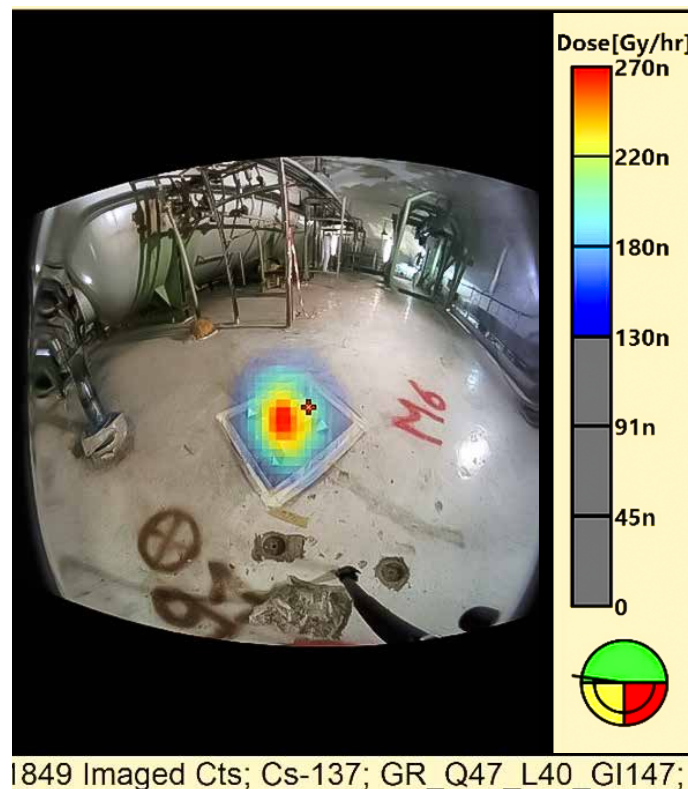


Figure 3: Example of 2D reconstruction of Cs-137 superimposed to the optical image. Courtesy of Nucleco spa.

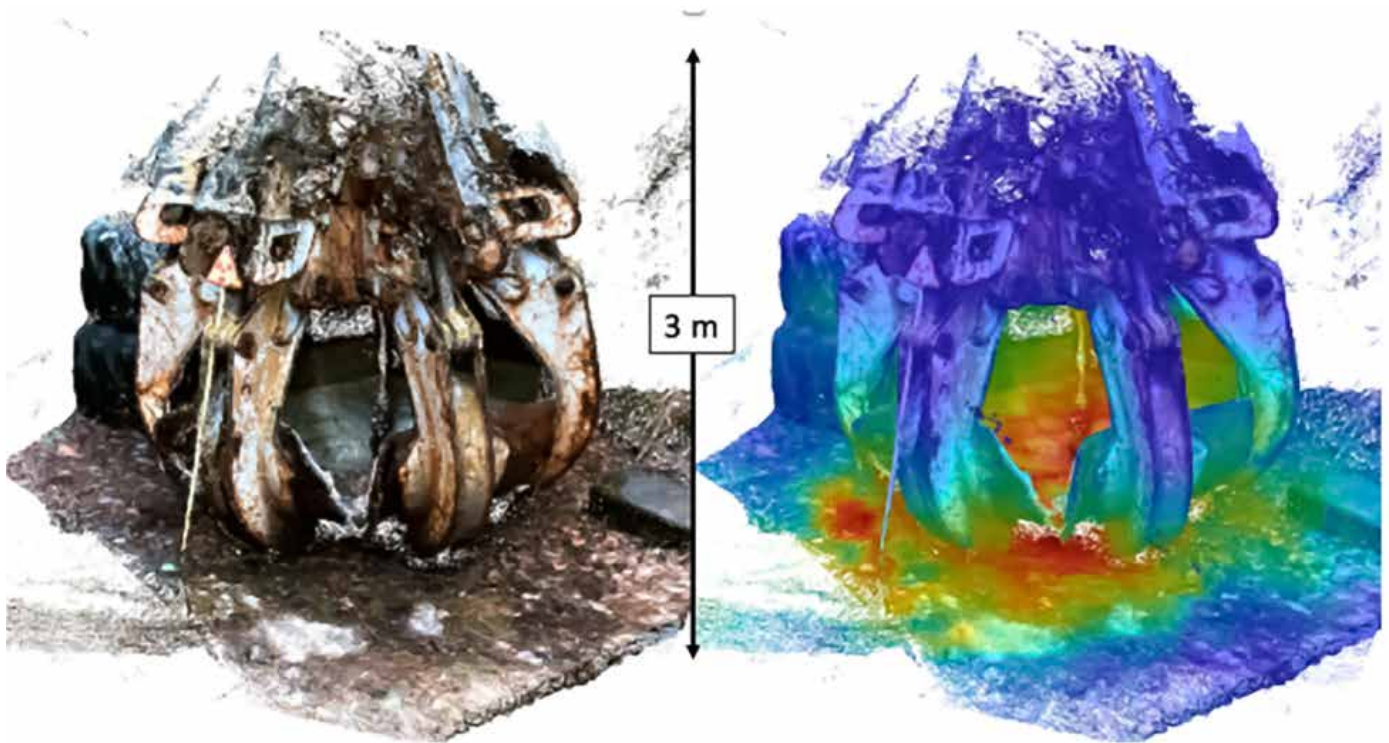


Figure 4: Photogrammetric reconstruction (left) of a claw located in forest outside Pripjat used in the aftermath of the Chernobyl accident. On the right, reconstruction of relative radiation level for Cs-137 (low level in blue, high level in orange and red) [25].

As a standalone device, gamma imaging systems typically provide the collected spectra and the 2D reconstruction of the gamma emitting radioactive material superimposed to the optical image acquired with a camera installed within the system (Figure 3). For the reconstruction, the system computes, for each recorded event, the most probable paths of the incident photons, and then sums them up in order to determine the most probable path of all the photons detected during the assay. These paths and their probabilities are exactly the data represented in Figure 3, which can thus be considered the real spatial distribution of the radioactive material emitting such photons.

The only way to reconstruct the distribution with a gamma imager without the external space physical information is using a 2D plane unless some well-known object and detector position are measured. However, the proposed Concept would allow a gamma camera to have access to SLAM data, i.e., knowing at a fixed rate its position and pose inside the 3D reconstruction of the space. This information can be used to extrapolate the probable directions for each event in a 3D space instead of a 2D plane, including corrections due to possible distance variations from the materials surrounding the system as it moves in space (see Figure 4). The information provided by the SLAM architecture permits a very appropriate evaluation of distances and interferences, being able to better distinguish among close hotspots of the same radionuclide and compute the distance-corrected quantification of the radioactivity present.

Regarding the algorithm used for computing the 3D radioactivity reconstruction, the most used is the Maximum Likelihood-Expectation Maximization (ML-EM) [19] with its variations, although it's known overfitting problems can arise and fixes are still under developments [20] [21]. However, other approaches do exist, ranging from easy-to-understand optical-like projection like the Filtered Simple Back Projection algorithm SBP [22], up to deep mathematical approaches like the Additive Point Source Localization APSL [23] [24].

In respect of just few years ago, two main improvements have been achieved by the most advanced imaging system:

- The capability to perform the imaging for a user-defined Region-Of-Interest (ROI), thus without any interference issue in imaging radionuclides having different gamma emissions (the energy resolution is crucial for this aspect).
- The capability to make quantitative evaluations of the radioactivity present. Not only CdZnTe can be used with Monte Carlo codes (like MCNP [26]), but also with point-kernel techniques for reliable radioactivity quantification [27]. Finally, the energy resolution allows the quantification of Uranium enrichment and Plutonium isotopic composition [28]. These results imply the possibility to apply a quantitative scale to the reconstruction.

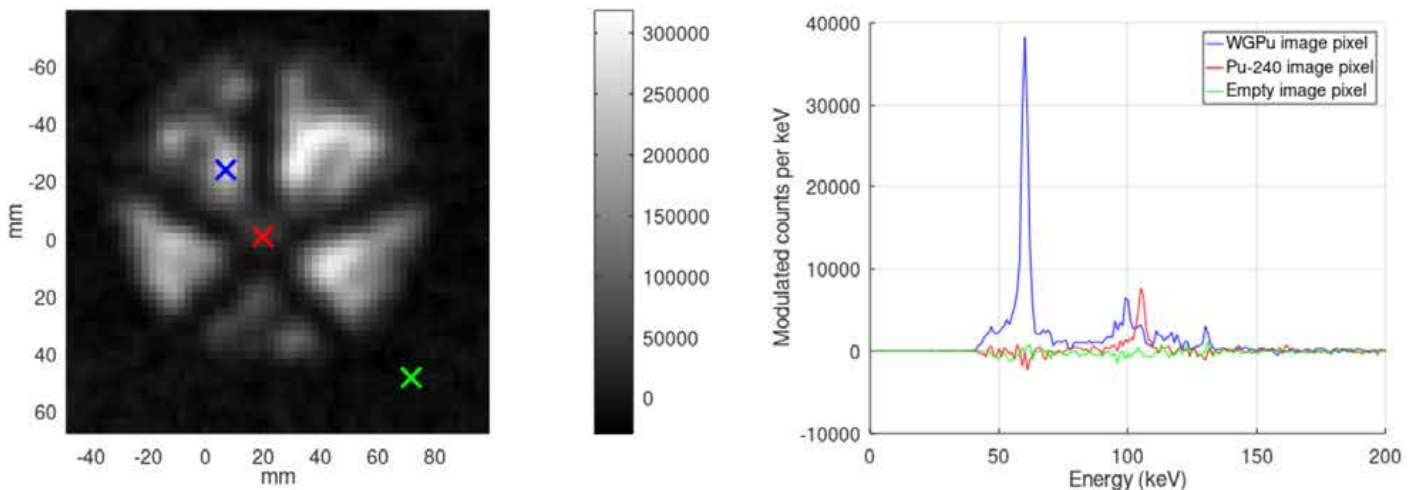


Figure 5: Example of direction spectrum: on the left, three pixels marked of a plutonium known sample, on the right the spectrum reconstructed from each marked pixel [29].

Finally, it's also to envisage the future possibility (under development [29] [30]) to retrieve directional spectra, i.e. to reconstruct (with a certain probability or fidelity) the spectrum generated by a certain hot spot emerging from a precise direction in the 3D model: this feature could potentially allow to drop the need to apply (sometime very large) collimation and shielding systems, resulting in a dramatic improvement in the imaging system versatility and operativity in standalone mode (example in Figure 5).

Regarding neutron imaging, current technology is mainly limited to using an active neutron flux to probe a certain material response [31] [32], in opposition to the passive approach used by gamma cameras. The need of an active flux is an important constraint in the application of this technique in portable devices, like the one used for in-situ inspections. However, some on-going studies (like [33] and [34]) demonstrate the possibility of performing a passive neutron imaging under certain conditions and coupling it with gamma imaging reconstruction, with results that might then be integrated into the 3D model. While waiting for this technology to be further developed, one can also use a rough neutron counter detector and apply the novacula Occami (Occam's blade) principle thanks to the SLAM-provided spatial awareness: as the neutron count rate grows when placing the counter close to an object than the object can be the source of that count rate. This approach has a simpler application and implementation but is much less precise than imaging and requires a deeper exploration of the space surrounding the item (requirement much more important for neutrons than for photons, because of their higher penetration power) in order to reduce interferences and false positives.

The dose rate can be measured by means of dedicated sensors or through the ones used for gamma/neutron imaging. Dose rate is mainly significative for radioprotection scopes (e.g., computing absorbed dose) thus it can be

more important to know it in a generic point of the 3D space than at contact with contaminated/activated items and nuclear materials. This goal is often reached running complex codes and resource-demanding particle transport simulations in an as-complete-as-possible 3D model of the entire facility with (at least) all the most important hot spots included in the model. Unfortunately, this approach can be harsh to implement and make almost no sense for facilities where conditions often change. In similar cases, it can have more sense to measure the dose rate in space and interpolate the results to get an heuristic dose rate field (which can be included into the 3D model as a hidden value) to be used for any possible radioprotection scope (like in [35]).

Regarding other possible radiological sensors, generally speaking, all possible detectors might be integrated to the Concept as long as their output can be referenced within the 3D model: an example is the application of radiation-tolerant RFID technology (like in [36]) for filling radiological data to the facility Common Data Environment.

3. From the Concept to the realization: the state-of-the-art

Nowadays the proposed Concept has few working physical realizations, almost all at the prototype state (examples in [37] and [38]). The Concept's core, the SLAM architecture, is usually based upon a LIDAR (for point-cloud creation) coupled with an odometry camera (for space-awareness), whilst the radiological data acquisition relies on CZT-based gamma imaging system coupled (when possible) with a Geiger-Muller for dose-rate measurement; nevertheless, differences are present among systems, from the sensors to the algorithms used for space and radioactivity reconstruction.

Although still missing a user-friendly managing software, the system presented in [39] and [40] (see Figure 6 and

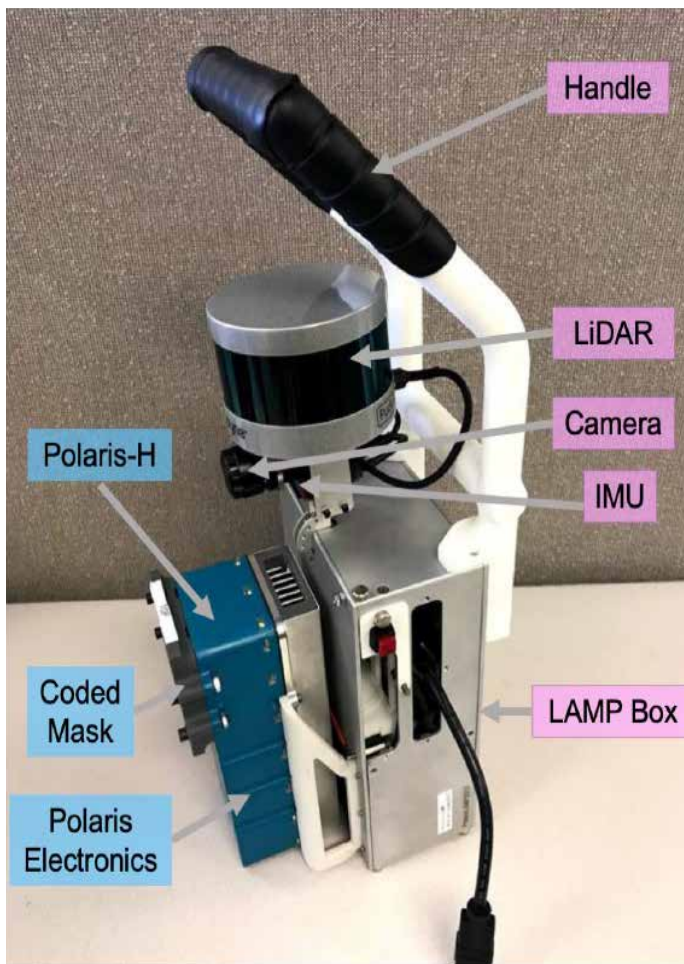


Figure 6: Polaris-LAMP system as proposed in [40]

Figure 7) appears to be most mature solution so far (in particular about the Scene Data Fusion topic), whose realization started several years ago and has reached the market recently [41]. Nevertheless, taking into account other factors, e.g. quantitative capability, managing software functionalities, computational and user effort required, the topic is far more complex and other solutions can be considered top-tiers: the system reported in [35] is equipped with an interesting software suite for radioprotection and augmented reality virtualization, whilst the system in realization reported in [42] shows enhanced quantification capabilities.

Regarding quantification capability, there are many on-going study to implement attenuation correction in the MLEM (or similar) reconstruction (which already correct for distance), thus retrieving the activity of each detected hotspot ([43][44][45]). Differently, in [42] the quantification is focused on using point-kernel based approach, similar to the worldwide-diffused commercial quantitative gamma spectrometers [46][47]. As already stated, other algorithms are under study and their application to SDF systems, like the Particle Swarming [48]. It's also worth to mention the study reported in [49] about the Minimum Detectable Activity (MDA) reached using systems like the Concept: similar evaluation would allow the user to understand the sensitivity of the assay performed as a function of the space in addition to distance (see Figure 8).

Finally, of high interest for safeguards and not proliferation is the possibility envisaged in [42] (based on previous work reported in [50]), and in [51] and [52], to apply space-aware imaging systems for 3D reconstruction and quantification in known items, in a sort of simplified (in the assumption but also in the requirement) tomography. It might be, in future, coupled with other tomographic system used for safeguards, like the PGET (Passive Gamma Emission Tomography) [53] [54].

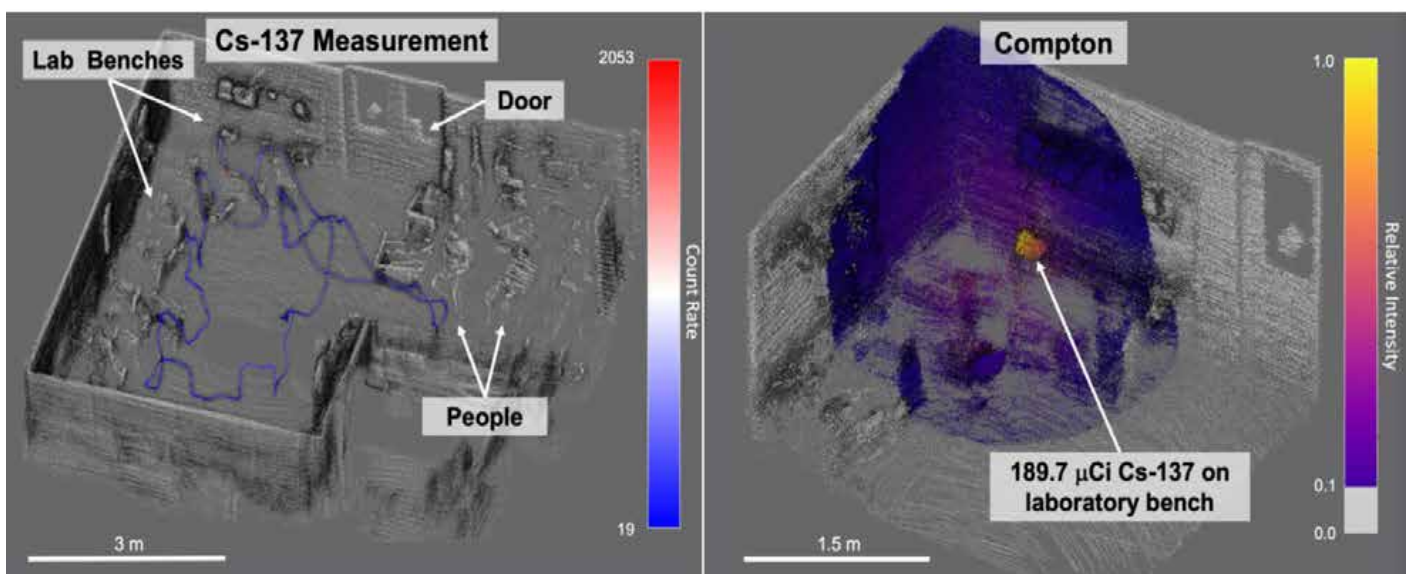


Figure 7: Application of Polaris-LAMP system: on the left, physical reconstruction of the environment with evidence of the travelled path; on the right, 3D radioactivity reconstruction using Compton Imaging [40].

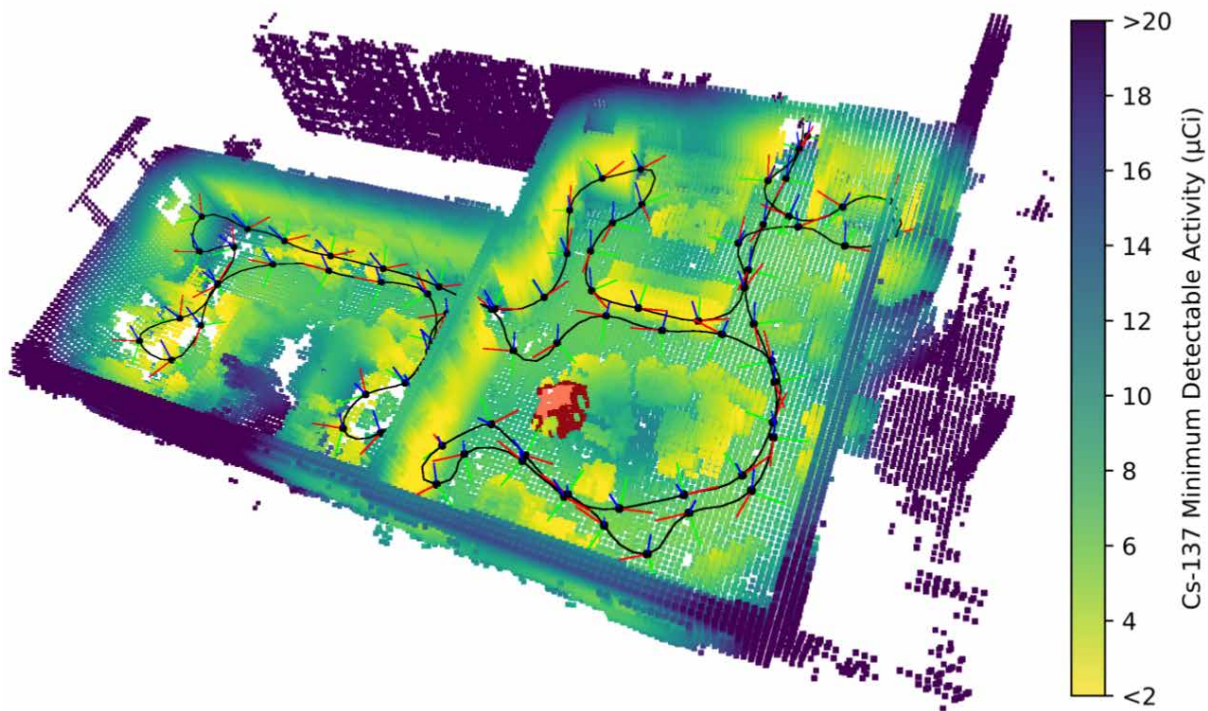


Figure 8: 3D view of MDA map for Cs-137 [49]

4. Application of the Concept to safeguards and beyond

As already mentioned, at the bare minimum the Concept will have a SLAM Architecture and a gamma imaging (capable of also evaluating the gamma dose rate). With minor effort, a neutron counter can be attached, initially without proper imaging capability. The Concept can be seen both as an integrated system or as several sensors and detectors which can be used separately for performing/optimizing specific tasks. At the present state, devices like the presented Concept are used to retrieve fast information about the position of a hot spot in a certain area, thus mainly from a radioprotection perspective.

As hand-held system, the Concept can be used to:

- ✓ Perform Design Information Verification activities, thanks to the possibility to compare the as-built 3D model from point cloud with the information declared by the user. That comparison can be extended to successive inspections to verify that nothing has changed in the facility without notification.
- ✓ During periodical inspections, to detect dose rate/gamma/neutron anomalies along the inspected installation, possible signature of SNM diverted from its scope. Thanks to the spatial awareness, the unexpected signature can be efficiently studied further with detailed measurements.

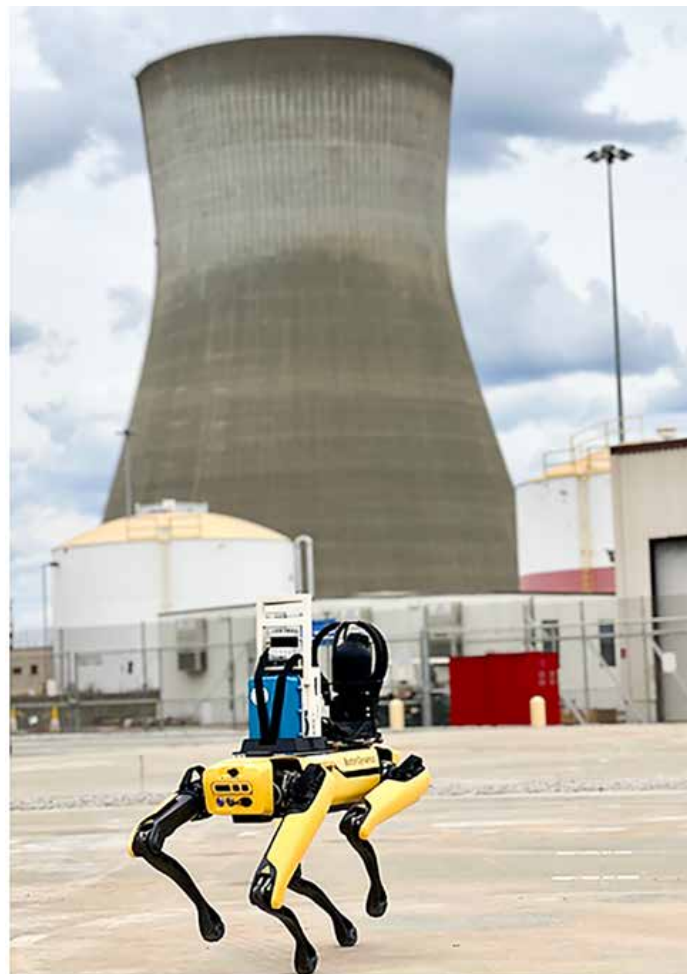


Figure 9: Example of imaging system installed on quadrupedal robotic platform during a routine assay.

- ✓ Quantify gross and partial mass defects and verify operators' declarations about Uranium enrichment, Plutonium isotopic composition, fuel burn-up and cooling time, with uncertainty similar to the one obtainable with portable HPGe.
- ✓ Collect multiple data to be used for radioprotection purposes (e.g., dose rate in air) and future radioactive waste management.

The Concept can also be used in a static mode like a monitoring system to preserve CoK between sequential inspections: during normal functioning, the system might elaborate and store the minimum data needed to identify eventual anomalies, whose detection enable the full-data acquisition. From the monitoring perspective, the Concept can be coupled to robotic systems in order to make autonomous acquisition along a pre-defined path (examples in [55] [56] [57] [58] [59]), in order to retrieve the same kind of information over time simplifying data management (Figure 9).

5. Conclusions

A Concept of an integrated system for creating 3D models and spatially aware radiological data has been introduced, reviewing what has been already developed and the improvements that the involved technologies may undergo in next future, making this kind of device of particular interest. In the perspective of safeguards and non-proliferation, the system can be seen as a multi-purpose device, whose complexity and cost are justified by the large amount of information obtainable without the need of other tools: in fact, it can be used not only for inspections, but also as (part of a) monitoring system and as a tool to keep track of spatially-aware and time-correlated physical and radiological quantities inside the facility, in order to complete its K-PIM description according to IAEA indications and preserve the Continuity of Knowledge.

6. Acknowledgements

The author would like to acknowledge the friend and colleague Luca Lionello for his patience in supporting and reviewing this manuscript.

7. References

- [1] Mihailescu L; Vetter K; Ruhter W; Chivers D; Dreicer M; Coates C, et al.; *Combined measurements with three-dimensional Design Information Verification system and gamma ray imaging - A collaborative effort between Oak Ridge National Laboratory, Lawrence Livermore National Laboratory and the Joint Research Center at Ispra*; article, June 14, 2006; Livermore, California. (<https://digital.library.unt.edu/ark:/67531/metadc883736/>: accessed August 31, 2022), University of North Texas Libraries, UNT Digital Library, <https://digital.library.unt.edu>; crediting UNT Libraries Government Documents Department.
- [2] International Atomic Energy Agency; *Application of Facility Information Models to manage design knowledge though the nuclear power facility life cycle*; IAEA-TECDOC-1919
- [3] Barnowski R, Haefner A, Mihailescu L, Vetter K; *Scene data fusion: Real-time standoff volumetric gamma-ray imaging*; Nucl. Instrum. Methods Phys. Res. Sec. A, Accel., Spectrom. Detectors Assoc. Equip., vol. 800, pp. 65–69, Nov. 2015.
- [4] Durrant-Whyte H, Bailey T; *Simultaneous localization and mapping: part I*; IEEE Robotics & Automation Magazine, vol. 13, no. 2, pp. 99-110, June 2006, doi: 10.1109/MRA.2006.1638022.
- [5] Hess W, Kohler D, Rapp H, Andor D; *Real-Time Loop Closure in 2D LIDAR SLAM*, in *Robotics and Automation (ICRA)*; 2016 IEEE International Conference on. IEEE, 2016. pp. 1271–1278.
- [6] Labbé M, Michaud F; *RTAB-Map as an Open-Source Lidar and Visual SLAM Library for Large-Scale and Long-Term Online Operation*; in *Journal of Field Robotics*, vol. 36, no. 2, pp. 416–446, 2019.
- [7] Campos C, Elvira R, Rodríguez J G, Montiel, J M, Tardós J D; *ORB-SLAM3: An Accurate Open-Source Library for Visual, Visual-Inertial, and Multimap SLAM*; in *IEEE Transactions on Robotics*, vol. 37, no. 6, pp. 1874-1890, Dec. 2021, doi: 10.1109/TRO.2021.3075644.
- [8] Yu X, He W, Qian X, Yang Y, Zhang T, Ou L; *Real-time rail recognition based on 3D point clouds*; *Measurement Science and Technology*, vol. 33, no. 10, 2022. doi:10.1088/1361-6501/ac750c.
- [9] Raimundo J, Lopez-Cuervo Medina S, Aguirre de Mata J, Prieto, J F; *Multisensor Data Fusion by Means of Voxelization: Application to a Construction Element of Historic Heritage*; *Remote Sens.* 2022, 14, 4172. <https://doi.org/10.3390/rs14174172>
- [10] Wahl C G et al.; *The Polaris-H imaging spectrometer*; *Nuclear Instruments and Methods in Physics Research A* 784 (2015) 377 – 381
- [11] Barnowski R, Haefner A, Vetter K; *LBNL's High Efficiency Multimodal Imager (HEMI) and Demonstration of Hand-Held Volumetric Imaging*; December 2015
- [12] Jablonowski E, Kiser M, Longford D, Mitchell J; *Application of the PHDS Germanium gamma-ray imager (GeGI) in facility decontamination assessment*; WM2019 Conference, USA

- [13] Montémont G et al.; *NuVISION: a Portable Multimode Gamma Camera based on HiSPECT Imaging Module*; 2017 IEEE Nuclear Science Symposium and Medical Imaging Conference (NSS/MIC), 2017, pp. 1-3, doi: 10.1109/NSSMIC.2017.8532713.
- [14] Amgarou K et al.; *A comprehensive experimental characterization of the iPIX gamma imager*; 2016 JINST 11 P08012
- [15] Hilsabeck J; *3D Gamma Source Mapping and Intervention Analysis*; WM2019 Conference, USA
- [16] Gottesman S, Fenimore E; *New family of binary arrays for coded aperture imaging*; *Appl. Opt.* 28, 4344-4352 (1989).
- [17] Hmissi M Z et al.; *First images from a CeBr3 /LYSO:Ce Temporal Imaging portable Compton camera at 1.3 MeV*; 2018 IEEE Nuclear Science Symposium and Medical Imaging Conference Proceedings (NSS/MIC), 2018, pp. 1-3, doi: 10.1109/NSSMIC.2018.8824429.
- [18] Lee H S, Kim J H, Lee J, Kim C H; *Development and performance evaluation of large-area hybrid gamma imager (LAHGI)*; *Nuclear Engineering and Technology*, Volume 53, Issue 8, 2021, Pages 2640-2645, ISSN 1738-5733, <https://doi.org/10.1016/j.net.2021.01.036>.
- [19] Wilderman S J, Clinthorne N H, Fessler J A, Rodgers W L; *List-Mode Maximum Likelihood Reconstruction of Compton Scatter Camera Images in Nuclear Medicine*; *IEEE Symposium on Nuclear Science*, 1998
- [20] Reader A J, Ellis S; *Bootstrap-optimised regularised image reconstruction for emission tomography*; *IEEE Trans. Med. Imag.*, vol. 39, no. 6, pp. 2163–2175, Jun. 2020
- [21] Bissantz N, Mair B A, Munk A; *A statistical stopping rule for MLEM reconstructions in PET*; in *Proc. IEEE Nucl. Sci. Symp. Conf. Rec.*, Oct. 2008, pp. 4198–4200.
- [22] Haefner A, Gunter D, Barnowski R, Vetter K; *A Filtered Back-Projection Algorithm for 4 π Compton Camera Data*; *IEEE Transactions on Nuclear Science*, vol. 62, no. 4, pp. 1911-1917, Aug. 2015, doi: 10.1109/TNS.2015.2457436.
- [23] Hellfeld D, Joshi T H Y, Bandstra M S, Cooper R J, Quiter B J, Vetter K; *Gamma-ray point-source localization and sparse image reconstruction using Poisson likelihood*; *IEEE Trans. Nucl. Sci.*, vol. 66, no. 9, pp. 2088–2099, Sep. 2019.
- [24] Vavrek J R et al.; *Reconstructing the Position and Intensity of Multiple Gamma-Ray Point Sources with a Sparse Parametric Algorithm*; *IEEE Transactions on Nuclear Science*, vol. 67, no. 11, pp. 2421-2430, Nov. 2020, doi: 10.1109/TNS.2020.3024735.
- [25] Vetter K; *Advances in Nuclear Radiation Sensing: Enabling 3-D Gamma-Ray Vision*; *Sensors*, 2019, 19(11):2541.
- [26] Werner C J, Bull J S, Solomon C J, et al.; *MCNP6.2 Release Notes*; LA-UR-18-20808, 2018.
- [27] Gagliardi F et al.; *Reliability of 3D Pixelated CdZnTe system in the quantitative assay of radioactive waste: a demonstration*; *IEEE Room Temperature Semiconductor Detector Conference*, 2022
- [28] Streicher M, Brown S, Zhu Y, Goodman D, He Z; *Special Nuclear Material Characterization Using Digital 3-D Position Sensitive CdZnTe Detectors and High Purity Germanium Spectrometers*; *IEEE Transactions on Nuclear Science*, vol. 63, no. 5, pp. 2649-2656, Oct. 2016, doi: 10.1109/TNS.2016.2593631.
- [29] Brown S et al.; *A Compact CdZnTe Coded Aperture Imaging Spectrometer for Isotopic Characterization*; *Proceedings of the INMM 59th Annual Meeting*, 2018
- [30] Brown S et al.; *A scanning coded-aperture imager for nuclear and radiological materials characterization*; *Proceedings of the INMM 63rd Annual Meeting*, 2022
- [31] International Atomic Energy Agency; *Neutron Imaging: A Nondestructive Tool for Materials Testing*; IAEA-TECDOC-1604, 2008.
- [32] Montague M, Hausladen P, Hayward J; *Proof-of-Concept Testing of a Modified Parallel-Slit Ring Collimator Neutron Imaging Tomography System for Spent Fuel Verification*; *IEEE Nuclear Science Symposium*, 2022.
- [33] Petrović J, Göök A, Cederwall B.; *Rapid imaging of special nuclear materials for nuclear nonproliferation and terrorism prevention*; *Sci Adv.* 2021 May 19;7(21):eabg3032. doi: 10.1126/sciadv.abg3032. PMID: 34138727; PMCID: PMC8133746.
- [34] Lopez R, Steinberger W M, Giha N, Marleau P, Clarke S D, Pozzi S A; *Neutron and gamma imaging using an organic glass scintillator handheld dual particle imager*; *Nuclear Instruments and Methods in Physics Research Section A: Accelerators, Spectrometers, Detectors and Associated Equipment*, Volume 1042, 2022.
- [35] McEntire J, McGee D; *Use of the Manuela 3D/Radiation Scanning Tool at Nuclear Facilities*; WM2020 Conference, USA.
- [36] Mini G, Morichi M, Pepe F, Rogo F; *Novel Platform for Digitization of Radiation Measurements, Decommissioning and Dismantling and Nuclear Waste Management*; WM2018 Conference, USA.
- [37] Rathnayaka P, Baek S H, Park S Y; *Stereo Vision-Based Gamma-Ray Imaging for 3D Scene Data Fusion*; *IEEE Access*, vol. 7, pp. 89604-89613, 2019, doi: 10.1109/ACCESS.2019.2926542.

- [38] Choi S, Lee J, Lee G, Kim D, Kim C H; *Real-time Contextual Data-Updated 3-D Radiation Image Reconstruction for Large-Area Hybrid Gamma Imager*; Transactions of the Korean Nuclear Society Spring Meeting, Jeju, Korea, May 19-20, 2022
- [39] Knecht K et al.; *Evaluating 3D Gamma-ray Imaging Techniques for Distributed Sources at the Fukushima Daiichi Nuclear Power Station*; IEEE Nuclear Science Symposium and Medical Imaging Conference (NSS/MIC), 2020, pp. 1-5, doi: 10.1109/NSS/MIC42677.2020.9507840.
- [40] Hecla J et al.; *Polaris-LAMP: Multi-Modal 3-D Image Reconstruction with a Commercial Gamma-Ray Imager*; IEEE Transactions on Nuclear Science, vol. 68, no. 10, pp. 2539-2549, Oct. 2021, doi: 10.1109/TNS.2021.3110162.
- [41] <https://www.gammareality.com/>
- [42] Goodman D et al.; *Radioactive Waste Localization, Identification, and Quantification using Spatially-Aware CdZnTe*; to be presented at WM2023 Conference, USA
- [43] Bandstra M S et al.; *Improved Gamma-Ray Point Source Quantification in Three Dimensions by Modeling Attenuation in the Scene*; IEEE Transactions on Nuclear Science, vol. 68, no. 11, pp. 2637-2646, Nov. 2021, doi: 10.1109/TNS.2021.3113588.
- [44] Hellfeld D, Bandstra M S, Vavrek J R et al.; *Free-moving Quantitative Gamma-ray Imaging*; Sci Rep 11, 20515 (2021). <https://doi.org/10.1038/s41598-021-99588-z>
- [45] Hellfeld D, Folsom M, Joshi T, Knecht K, Lee J, Gunter D, Schmitt K, Daughhetee J, Ziock K, Horne S, Brown S, Goodman D; *Quantitative Compton Imaging in 3D*; Proceedings of the INMM 63rd Annual Meeting, 2022, United States
- [46] Venkataraman R, Bronson F, Abashkevich V, Young B M, Field M; *Validation of in situ object counting system (ISOCS) mathematical efficiency calibration software*; Nuclear Instruments and Methods in Physics Research Section A: Accelerators, Spectrometers, Detectors and Associated Equipment, Volume 422, Issues 1-3, 1999
- [47] Abbas D K, Simonelli F, D'Alberti F, Forte M, Stroosnijder M F; *Reliability of two calculation codes for efficiency calibrations of HPGe detectors*; Applied Radiation and Isotopes, Volume 56, Issue 5, 2002
- [48] Parvin D, Clarke S; *Particle Swarm Imaging (PSIM). A swarming algorithm for the reporting of robust, optimal measurement uncertainties*; ESARDA Bulletin, 41-52, 2015
- [49] Bandstra M S, Hellfeld D, Lee J, Quiter B J, Salathe M, Vavrek J R, Joshi T H; *Mapping the Minimum Detectable Activities of Gamma-Ray Sources in a 3-D Scene*; arXiv preprint arXiv:2208.03321, 2022
- [50] Kaye W, Wang W, Kitchen B; *Waste Characterization Methods Based on Gamma-ray Imaging Spectrometers*; WM2019 Conference, USA
- [51] Hmissi Z et al.; *Passive Isotope Specific Gamma Ray Tomography of a Nuclear Waste Drum using a CeBr3 Compton Camera*; International conference on Advancements in Nuclear Instrumentation Measurement Methods and their Applications, Prague, Czech Republic, 2021.
- [52] Hmissi Z et al.; *3D Compton tomography from sparse views of a nuclear waste drum: Possible implication for legacy waste analysis*, IEEE Nuclear Science Symposium, 2022
- [53] Fang M, Altmann Y, Della Latta D et al.; *Quantitative imaging and automated fuel pin identification for passive gamma emission tomography*; Sci Rep 11, 2442 (2021). <https://doi.org/10.1038/s41598-021-82031-8>
- [54] Dendooven P, Virta R, Bubba T A, Moring M, Siltanen S, Honkamaa T; *Improved Passive Gamma Emission Tomography of the Center of Spent Nuclear Fuel Assemblies*; IEEE Nuclear Science Symposium, 2022
- [55] Pavlovsky R et al.; *3D Gamma-ray and Neutron Mapping in Real-Time with the Localization and Mapping Platform from Unmanned Aerial Systems and Man-Portable Configurations*; arXiv: Instrumentation and Detectors (2019)
- [56] Sato Y et al.; *Remote detection of radioactive hotspot using a Compton camera mounted on a moving multi-copter drone above a contaminated area in Fukushima*; Journal of Nuclear Science and Technology, 2020, 57:6, 734-744, DOI: 10.1080/00223131.2020.1720845
- [57] Friedman M, Mellor M, Murcutt P, Fallon M, Havoutis I, Casseau B; *A Modular Sensor Package for Autonomous 3D Gamma Mapping and Dose Management*; WM2021 Conference, USA
- [58] McGrath R, Kim-Stevens K; *EPRI Demonstration of an Autonomous Drone at Peach Bottom NPP*; WM2021 Conference, USA
- [59] Bondin M, Cheng R, Shurley A, Lee J, Zerza A, Ford M, Zaitseva N P, Vetter K; *Radioactivity Mapping using Small Unmanned Aerial Systems Composed of Active-Structural 6Li-PSD Plastic Scintillators*; IEEE Nuclear Science Symposium, 2022

